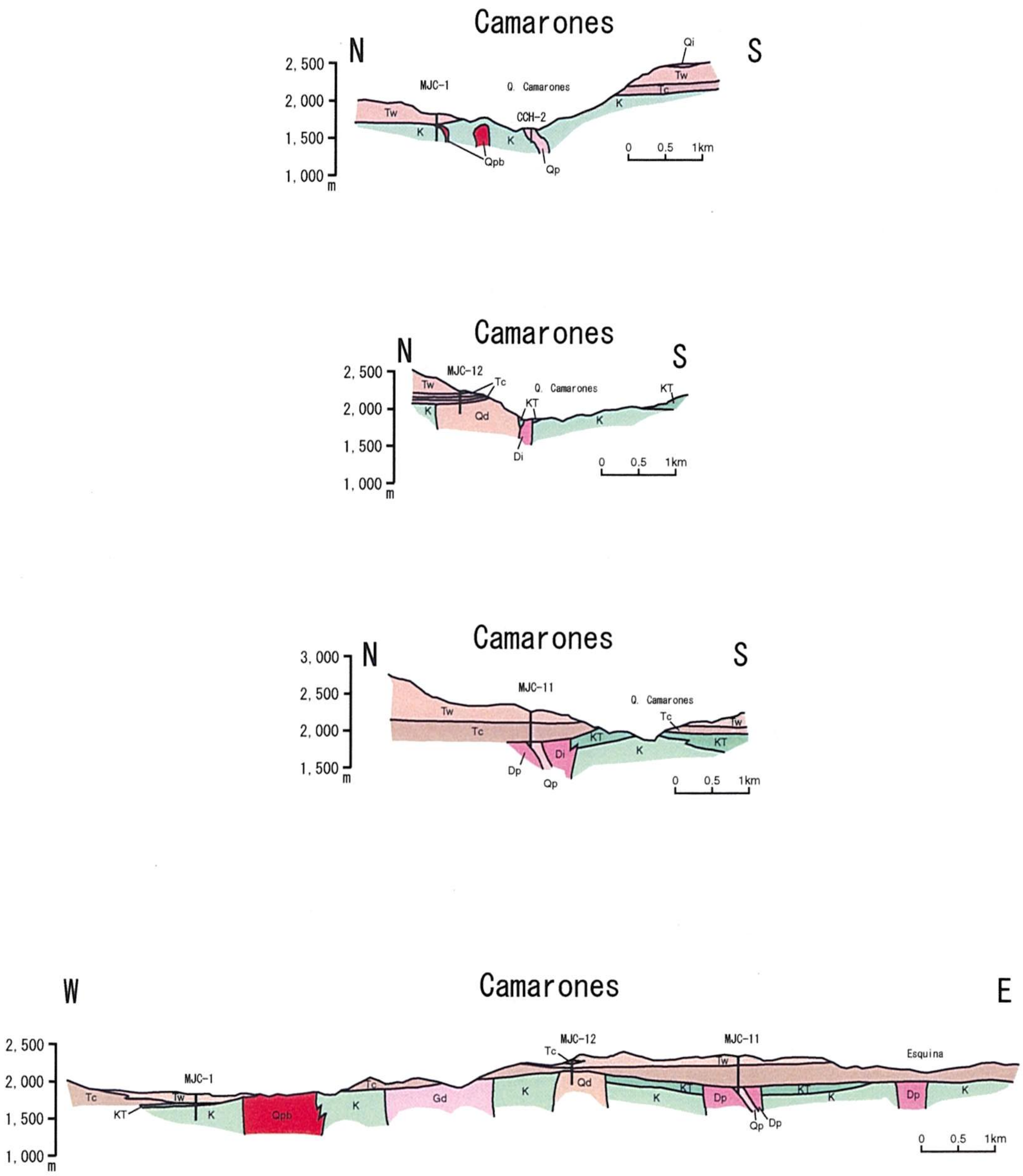

Fig. 2-2-3 Geological Profiles of the Camarones Area

The quartz porphyritic breccia is sericitized with cataclastic texture and is oxidized to reddish brown.

The ignimbrite is purplish gray to brown and consists of quartz-biotite-bearing rhyolitic welded tuff. Conglomerate below the ignimbrite is lacking in this hole, and thus this ignimbrite is inferred to be a landslide deposit.

② Alteration-mineralization

The quartz porphyritic breccia and andesite below 136m depth have been sericitized and silicified and is accompanied by chloritization below 185m depth.

The quartz porphyritic breccia has been strongly limonitized in 136~142m depth interval and this is an oxidized zone. Also relatively strong pyrite dissemination occurs in the quartz porphyritic breccia and andesite below 142m depth. Copper minerals could not be identified by unaided eyes in this hole. Copper content is somewhat larger below 306m compared to the upper part (Fig. 2-2-4).

MJC-11

① Geology

The geology of this hole consists of, from bottom upward, Upper Cretaceous-Paleogene diorite porphyry・quartz porphyry, Miocene conglomerate and Miocene-Pliocene ignimbrite.

The diorite porphyry is dark gray, and is sericitized and chloritized and accompanied by pyrite dissemination.

Quartz porphyry is white to gray and contains large quartz phenocrysts (3-5mm).

The conglomerate consists of quartz diorite, quartz porphyry, granodiorite, andesite, silicified rock, tuffaceous sandstone pebbles, and contains intercalation of thin white to pink volcanic ash layers.

The ignimbrite is red to purplish gray and consists of quart-biotite-bearing welded tuff.

② Alteration-mineralization

Quartz porphyry and diorite porphyry are strongly sericitized and silicified below 428m depth.

The quartz porphyry below 456m depth is oxidized and is limonitized, and relatively strong pyrite dissemination is observed in quartz porphyry and diorite porphyry below 456m depth. It was not possible to identify copper minerals by unaided eyes in this hole. Also the assay indicated low grade (Fig. 2-2-4).

MJC-12:

① Geology

The geology of this hole consists of Upper Cretaceous-Paleogene quartz diorite, Miocene conglomerate, Miocene-Pliocene ignimbrite, and Quaternary gravel.

The quartz diorite is dark green, and is chloritized and epidotized.

The conglomerate contains quartz diorite pebbles, and intercalation of thin silt~sandstone layers and pumiceous tuff layers.

The ignimbrite is reddish brown, and consists of dacitic pumiceous tuff and quartz·biotite -bearing rhyolitic welded tuff.

The Quaternary gravel layer contains intercalation of ignimbrite, but it is considered to be a landslide deposit.

② Alteration-mineralization

Quartz diorite below 164m depth is relatively strongly propylitized and partly sericitized with weak pyrite dissemination.

Copper minerals could not be identified by unaided eyes, but assay indicated relatively high Cu background value (Fig. 2-2-4).

(5) Minimiñe area (MJC-9)

A geological map of the area is shown in Figure 2-1-32 and geological cross section in Figure 2-1-33.

MJC-9:

① Geology

The geology of this hole consists of, from bottom upward, Miocene-Pliocene ignimbrite, Upper Neogene-Quaternary conglomerate and ignimbrite, and Pleistocene-Holocene gravel and talus deposits.

The Miocene-Pliocene ignimbrite is pink to gray, and consists of quartz-biotite-bearing rhyolitic welded tuff with intercalation of thin crystalline tuff beds.

The Upper Neogene-Quaternary conglomerate is dark gray to brown, and consists of andesitic~dacitic pebbles with in intercalation of crystalline tuff and pumiceous tuff beds in the upper part.

The Upper Neogene-quaternary ignimbrite is pink to brown, and consists of quartz-biotite-rich rhyolitic welded tuff.

The Pleistocene-Holocene gravel and talus deposits consist of andesitic~dacitic pebbles, crystalline tuff and pumiceous tuff blocks.

② Alteration-mineralization

Notable alteration and mineralization are not found in this hole, only sericitization is partly observed below 484m depth.

(6) Area to the northeast of Camiña area (MJC-10)

A geological map of the area is shown in Figure 2-1-28 and geological cross section in Figure 2-1-29.

MJC-10:

① Geology

The geology of this area consists of Upper Neogene-Quaternary basalt lava and alluvium.

The basalt lava is dark gray and aphyric. Strongly altered rocks are intercalated in various places.

The alluvium is thinly distributed over a wide area consisting of pebbles and sand.

② Alteration-mineralization

Strong argillization consisting of kaolin-smectite is widely developed in this hole, and is partly silicified.

Limonite dissemination occurs in 14~24m depth interval, and fine-pyrite dissemination below 36m depth. Cu-As-Hg anomalies are observed in the alteration zone in 14~36m and 68~82m depth intervals (Fig. 2-2-4).

2-5 Magnetic Anomalies and Geology and Mineralization

Of the 12 holes drilled in the overlap zones of intermediate airborne magnetic intensity zones and the peripheries of the medium wavelength anomaly zones, three (MJC-1, 11, 12) in Camarones area reached the porphyry-copper horizon of pre-Early Oligocene formation (pre-Lower Oligocene Series). MJC-1 and MJC-12 caught brecciated intrusive body and intrusive igneous body which are of the same nature as the igneous rocks related to porphyry copper mineralization, namely quartz porphyry. Also strong pyrite mineralization was confirmed in these holes. At MJC-12, quartz diorite believed to be of Eocene activity was confirmed and weak pyrite mineralization was confirmed.

On the other hand, the nine holes in areas other than Camarones, were drilled through Oligocene-Miocene conglomerate or younger formations. Of these, MJC-8 of Arica and MJC-2 of Codpa were drilled through Oligocene-Miocene conglomerate and approached pre-Oligocene units.

From geology of the holes and the magnetic susceptibility of the cuttings, regular relation between the basement depth and the airborne medium wavelength anomalies or short wavelength anomalies could not be found. In Camarones, the reason for reaching the pre-Lower Oligocene units was the short distance – less than 1km – from the pre-Lower Oligocene area on the surface.

The general trend of the variation of magnetic susceptibility of the cuttings can be correlated to the geology and alteration of the drill holes. Namely, it is stronger in mafic igneous rocks, and that of the Tertiary and Neogene-Quaternary conglomerate is higher than that of pyroclastic rocks and shallow gravel beds. Also the magnetic susceptibility is relatively low in phyllic alteration zones, acidic alteration zones and oxidized zones while it is higher in propylitic alteration zones.

It is believed that the possibility of reaching porphyry-copper type mineralized-altered zones in the two drill holes of Camarones area, and the drill hole in Northeast of Camiña area

(MJC-10) reached epithermal type mineralization alteration zone in Tertiary-Quaternary igneous bodies. It is believed to be possible that magnetic anomalies are closely related to igneous bodies and alteration, but as the number of drill holes reaching pre-Lower Oligocene units are small, it is not possible at this stage to confirm the relation between magnetic anomalies and porphyry-copper type mineralization and alteration. Also since mineralization is not observed in MJC-6 and 7 which have relatively similar geologic environment to MJC-10, there must be other factors controlling epithermal type mineralization and alteration other than the above magnetic anomalies (intermediate magnetic intensity zone and peripheries of the medium wavelength anomaly zones).

MJC - 1A

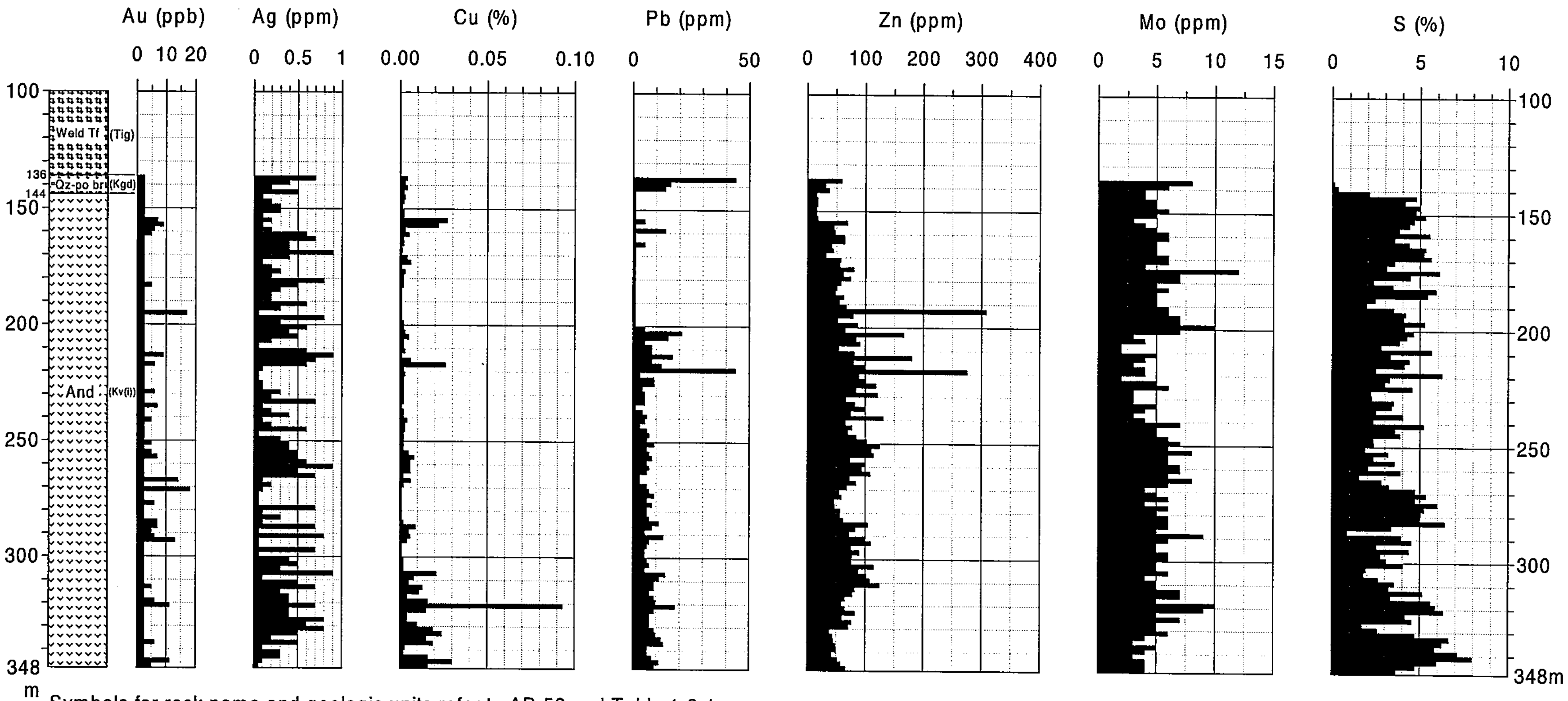

Symbols for rock name and geologic units refer to AP-53 and Table 1-3-1

Fig. 2-2-4 Histogram of Assay Results of Drill Holes (MJC-1A)

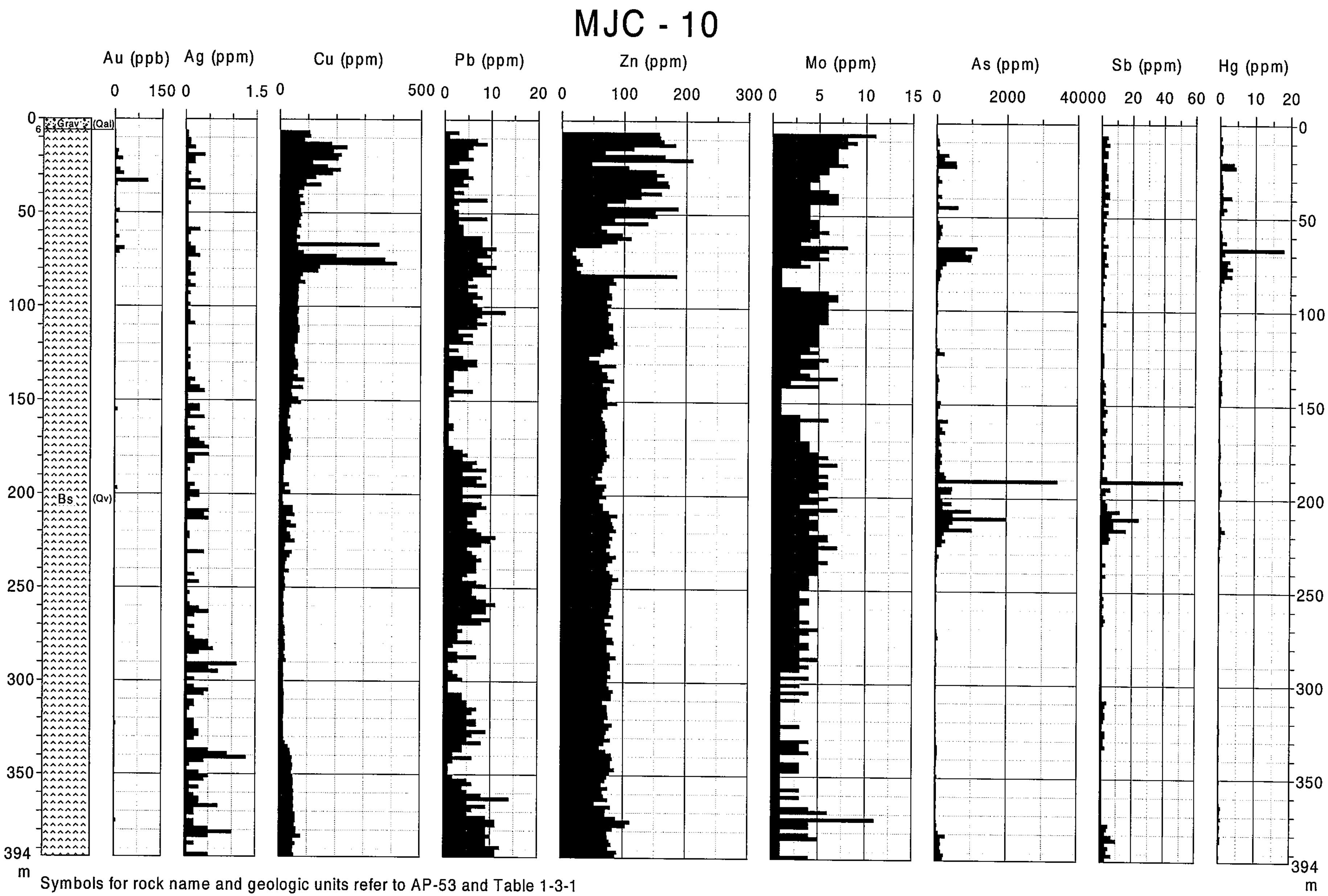

Fig. 2-2-4 Histogram of Assay Results of Drill Holes (MJC-10)

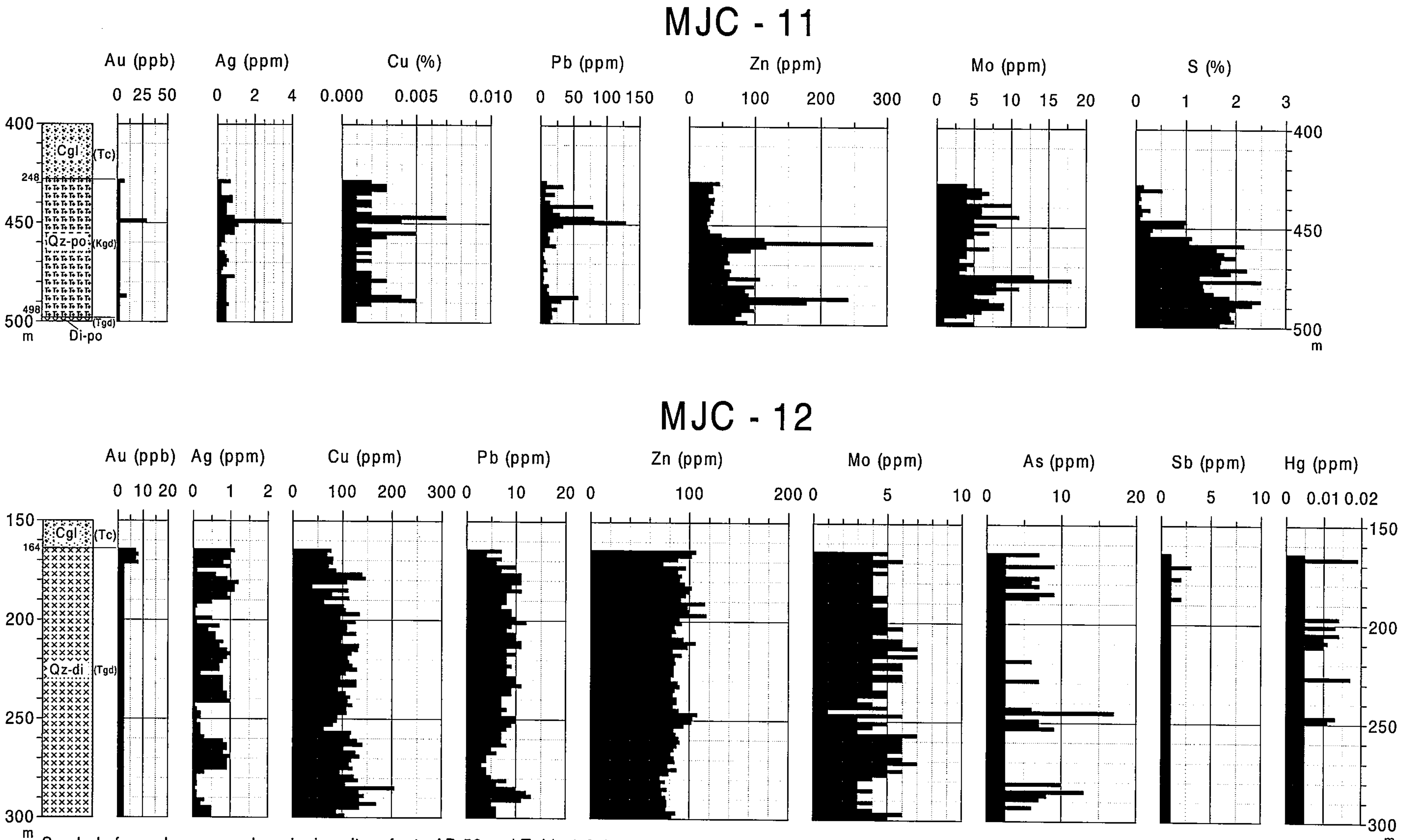

Symbols for rock name and geologic units refer to AP-53 and Table 1-3-1

Fig. 2-2-4 Histogram of Assay Results of Drill Holes (MJC-11,MJC-12)

CHAPTER 3 RE-ANALYSIS OF AIRBORNE MAGNETIC DATA

CODELCO has shown that high macroscopic correlation exists between the major porphyry copper deposits of northern Chile and transverse magnetic anomalies. This fully applies to the major porphyry copper deposits in the central to southern parts of Region I. But transverse magnetic anomalies are not clear in the northern part (See Figure 2-3) , and thus in the present survey investigation was not to limited to transverse magnetic anomalies, but all magnetic anomalies were analyzed and examined. Frequency analysis was adopted in order to consider the relation between porphyry copper deposits and magnetic anomalies in the level of individual anomalies.

A flowchart of the re-analysis work of the airborne magnetic data is laid out in Figure 2-3-1. Data acquisition, compilation of existing data, preparation of magnetic maps, magnetic structure analysis, and preliminary two-dimensional modeling were carried out during the second year of this project. Thus during the third year, magnetic susceptibility and remanent magnetism were measured for the entire Region I area, many magnetic anomalies were extracted by frequency analysis, and the results were evaluated for porphyry copper exploration.

3-1 Airborne Magnetic Data

The total magnetic intensity (TMI) map used for the analysis is shown in Figure 2-3-2. The sources of the airborne magnetic data used for the preparation of this map are laid out in Figure 2-3-3. A magnetic map (RTP map) prepared by reducing TMI to the pole is shown in Figure 2-3-4. This map was used for the analyses and interpretations except two-dimensional modeling. The results of magnetic structure analysis carried out during the second year is shown in Fig.2-3-5. Obtained magnetic structures are summarized as follows.

①The tectonic overview highlights the subdivision of the region into several tectonic subdomains: a regional migration of magmatic activity can be traced west to east. The western Cretaceous La Negra / Coastal Batholith magmatic arc was superseded by the interpreted Palaeocene, Tarapaca Back Arc magmatic belt. Further east, the deformed Mesozoic sediment / volcanic sequences and eastern Palaeozoic basement were intruded by early-mid Tertiary (porphyry-related) intrusives. These were superseded by a weakly-discordant series of Mid-Tertiary to Recent volcanic centres (trending NNW). The main early-Tertiary intrusive complexes also follow a NNW discordant structural trend.

②The various subdomains define a roughly N-S regional grain for the Andean Belt, with a significant bend towards the NNW north of ~20°S (coincident with Tertiary-Quaternary magmatism). Several major NW, NE and E-W transfer fault zones or corridors are highlighted in the regional structure. These have been active during several deformational episodes, and have played a major role in focussing both mineralised porphyry and epithermal systems within this region, and throughout the rest of the Andean Belt.

③The northern continuation of several crustal-scale orogen - parallel fault systems associated with major mineralisation throughout Central and Northern Chile have been interpreted from the magnetic data, includeing the Domeyko Fault System (DFS). This structure is related to the western fault margin of Palaeozoic basement, and is the regional structural locus for the giant Cu porphyries at Escondida, El Salvador, Chuquicamata, Collahuasi, Quebrada Blanca (and others). A series of subvolcanic intrusive and caldera structures have also been interpreted from the data: many of these are coincident with both known mineralisation and regional structures.

④A series of target zones have been selected for both porphyry Cu and epithermal / volcanic dome related Au/Ag mineralisation. These targets are based on associations of confluence of regional structures, localised and regional magnetic characteristics, and distribution of known mineralisation. The most prospective exploration districts occur within 4 significant zones, spaced approximately 80km apart, along a subtle NNW trending structural corridor (these include the districts hosting Collahuasi and Cerro Colorado).

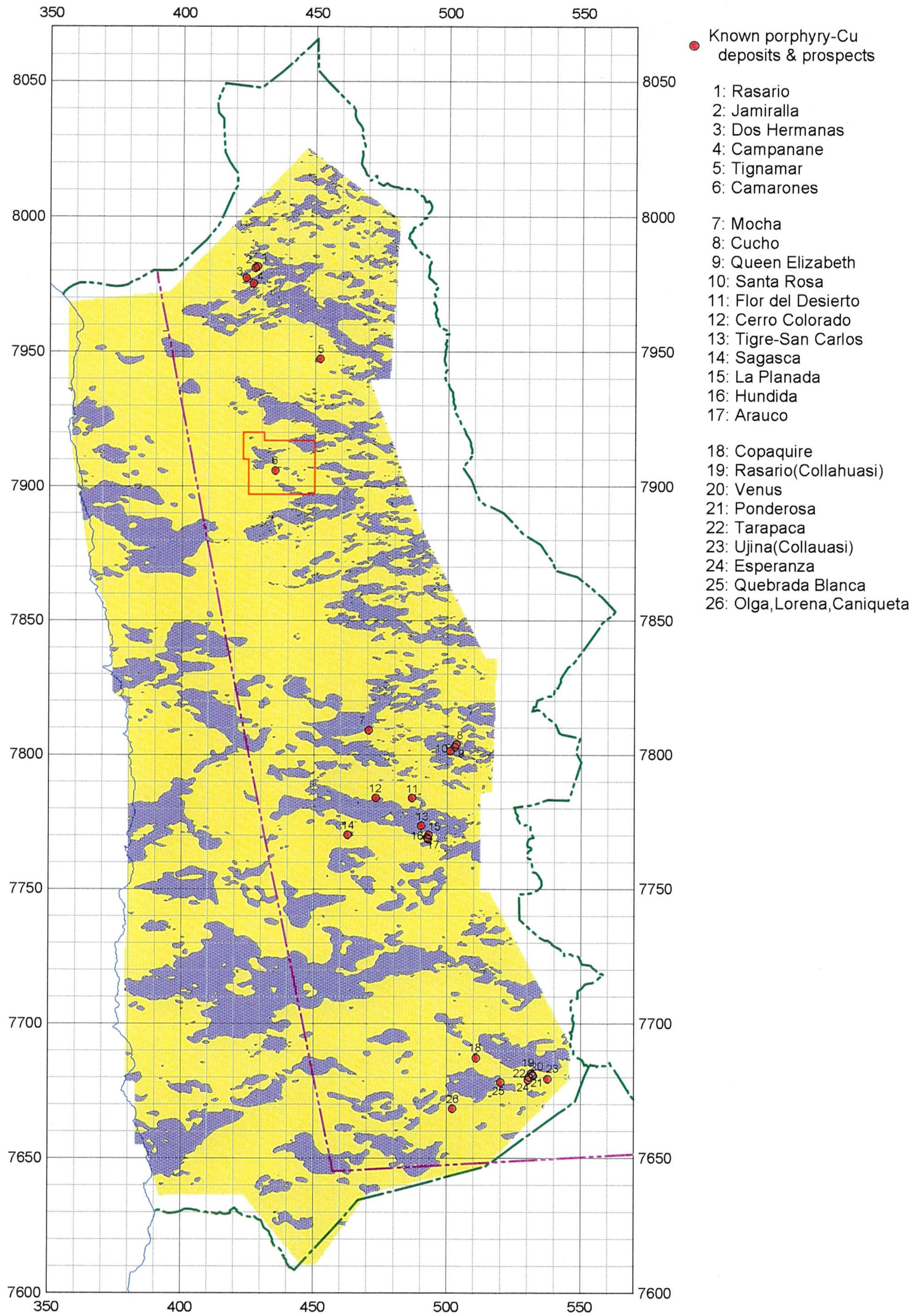

Fig. 2-3 Transverse Magnetic Anomalies and Known Porphyry-Cu Deposits & Prospects

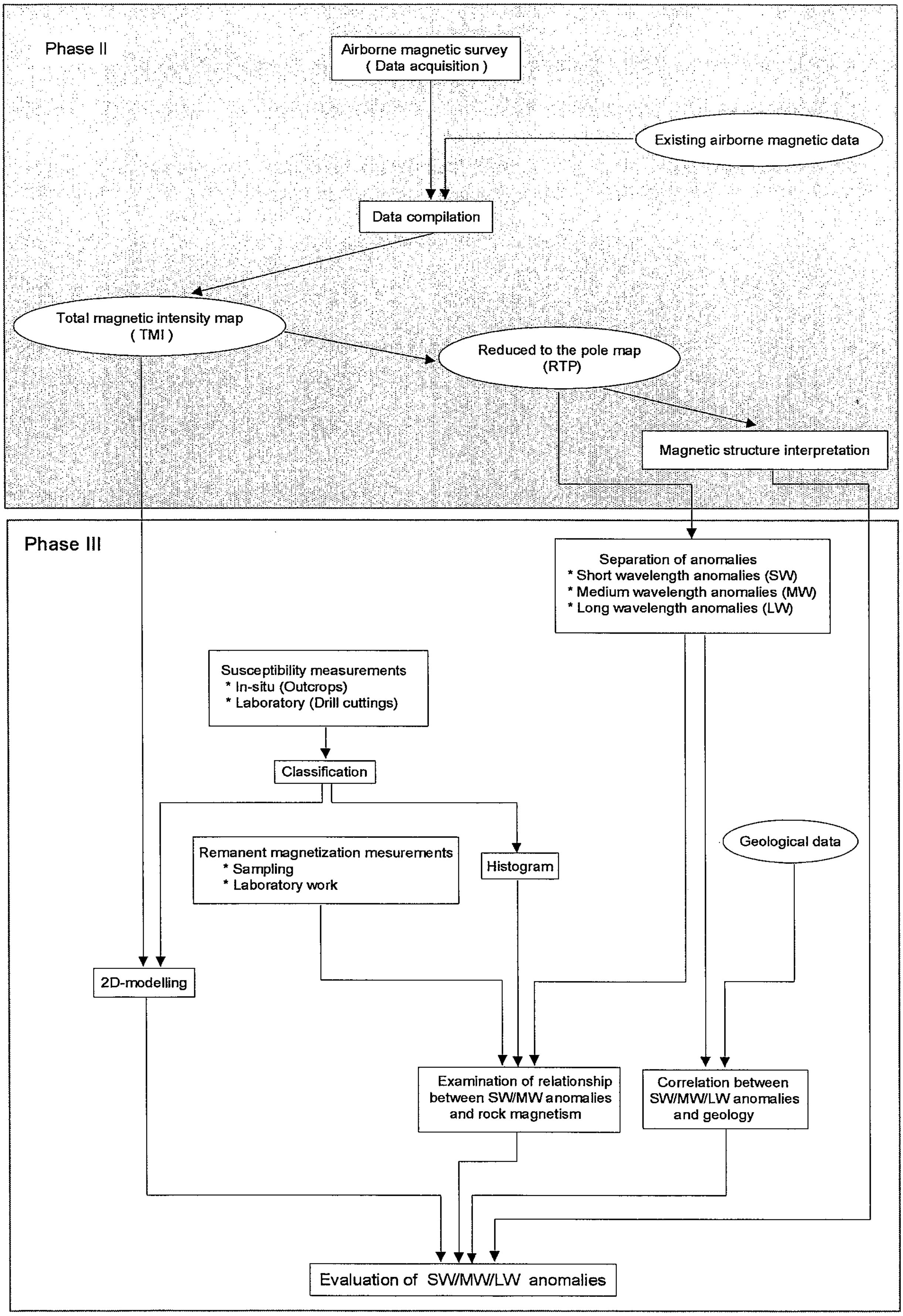

Fig. 2-3-1 Flowchart of Airborne Magnetic Interpretation

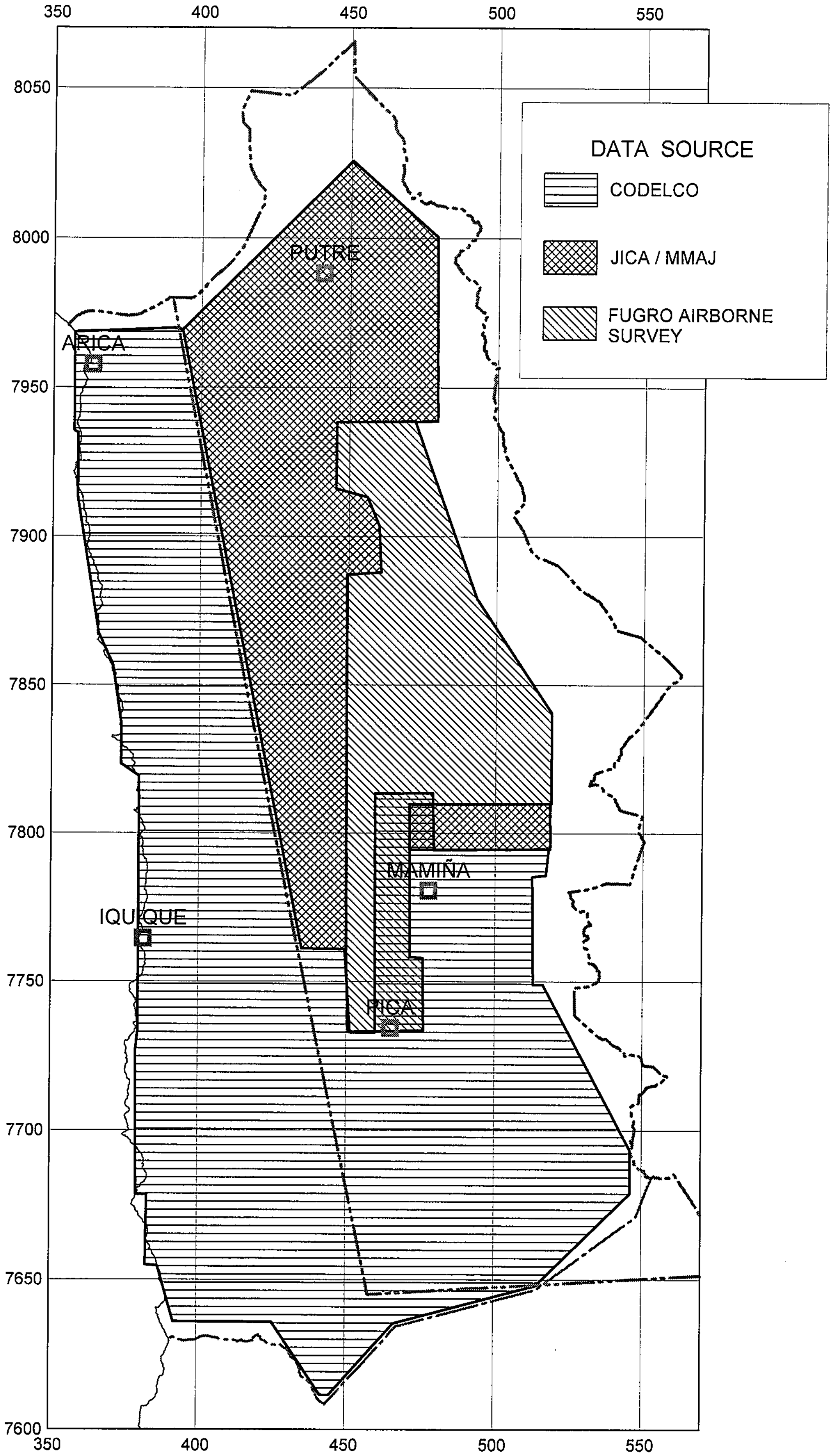

Fig.2-3-2 Airborne Magnetic Data Source

3-2 Separation of Magnetic Anomalies

RTP map shows magnetic anomalies formed by overlapping anomalies of various sizes. Frequency analysis was carried out with the purpose of separating these anomalies in order to distinguish them as independent magnetic anomalies. First, 6 kinds of RTP maps were prepared by extracting magnetic anomalies larger than; 4km, 7km, 12km, 17km, 24km, and 33km by high-cut filters. Then 4 kinds of RTP maps were prepared by extracting anomalies with sizes; 4~7km, 4~12km, 12~24km, and 12~33km by band-pass filters.

The magnetic anomalies which appear on these 10 maps and the location of the 26 known porphyry copper type mineralized zones were examined. The results indicated a close relation between the porphyry copper type mineralized zones and the 12~24km-size magnetic anomalies. The following three kinds of RTP maps were prepared on the basis of this result.

- short wavelength RTP map: anomalies over 12km were removed
- medium wavelength RTP map: anomalies over 24km and under 12km were removed
- long wavelength RTP map: anomalies under 24km were removed

These maps are laid out in Figures 2-3-6 to 2-3-8.

Next, each magnetic anomaly was distinguished and extracted from the above three RTP maps. The extracted magnetic anomalies are shown in the magnetic anomaly distribution maps laid out in Figures 2-3-9 to 2-3-11. Anomalies with RTP value of more than 60 ~ 80nT at the center of anomaly were extracted.

For short wavelength and medium wavelength magnetic anomalies, each extracted anomaly was sequentially numbered, and the coordinates, intensity, geologic information of the locality, access, and other relevant information were recorded in a inventory of SW/MW magnetic anomaly respectively. As for the long wavelength anomalies, they were only sequentially numbered.

The inventories of magnetic anomaly were prepared before the surface survey, and their geological and access information was useful for the selection of the sites for magnetic susceptibility measurements for the entire Region I area. These inventories are appended as AP-54 and AP-55.

Overlay maps of short, medium, and long wavelength magnetic anomaly distribution, reduced to the pole magnetism and porphyry copper mineralized zones are laid out in Figures 2-3-12 to 2-3-17. It is seen from Figure 2-3-16 that, with the exception of the 4 localities west of Putre, 22 known porphyry copper mineralized zones out of 26 localities lie within or in the vicinity of medium wavelength anomalies.

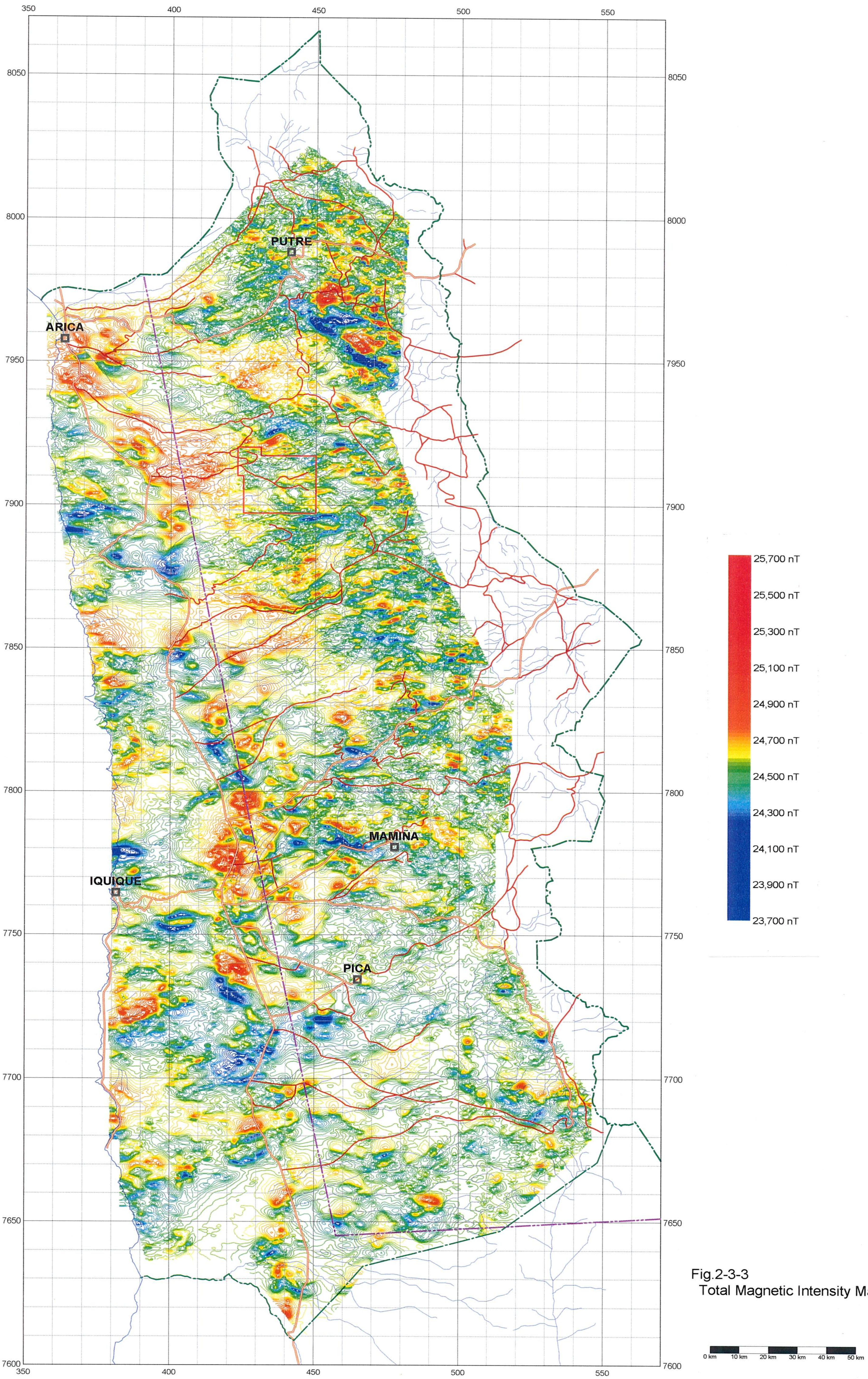

Fig.2-3-3
Total Magnetic Intensity Map

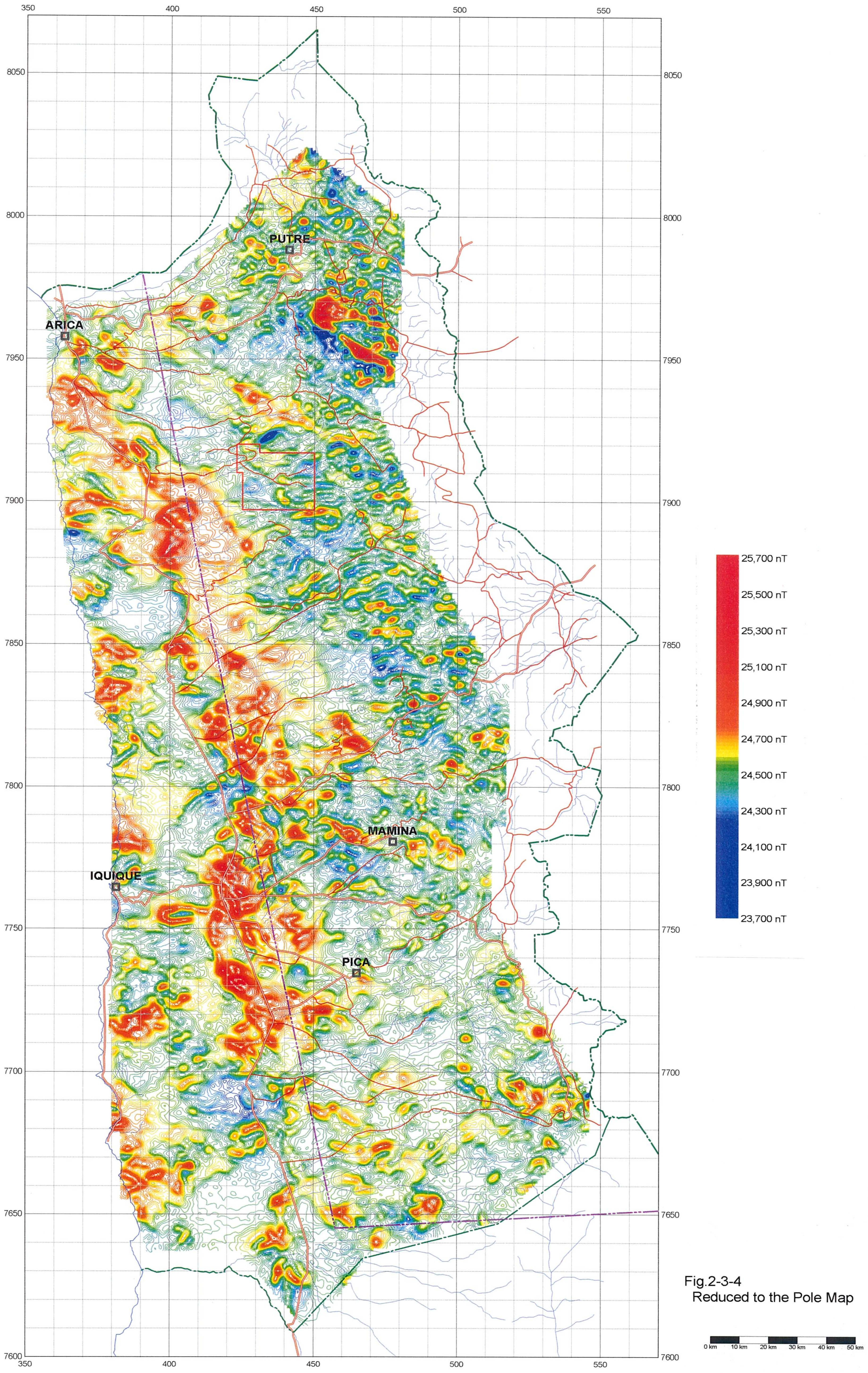

Fig.2-3-4
Reduced to the Pole Map

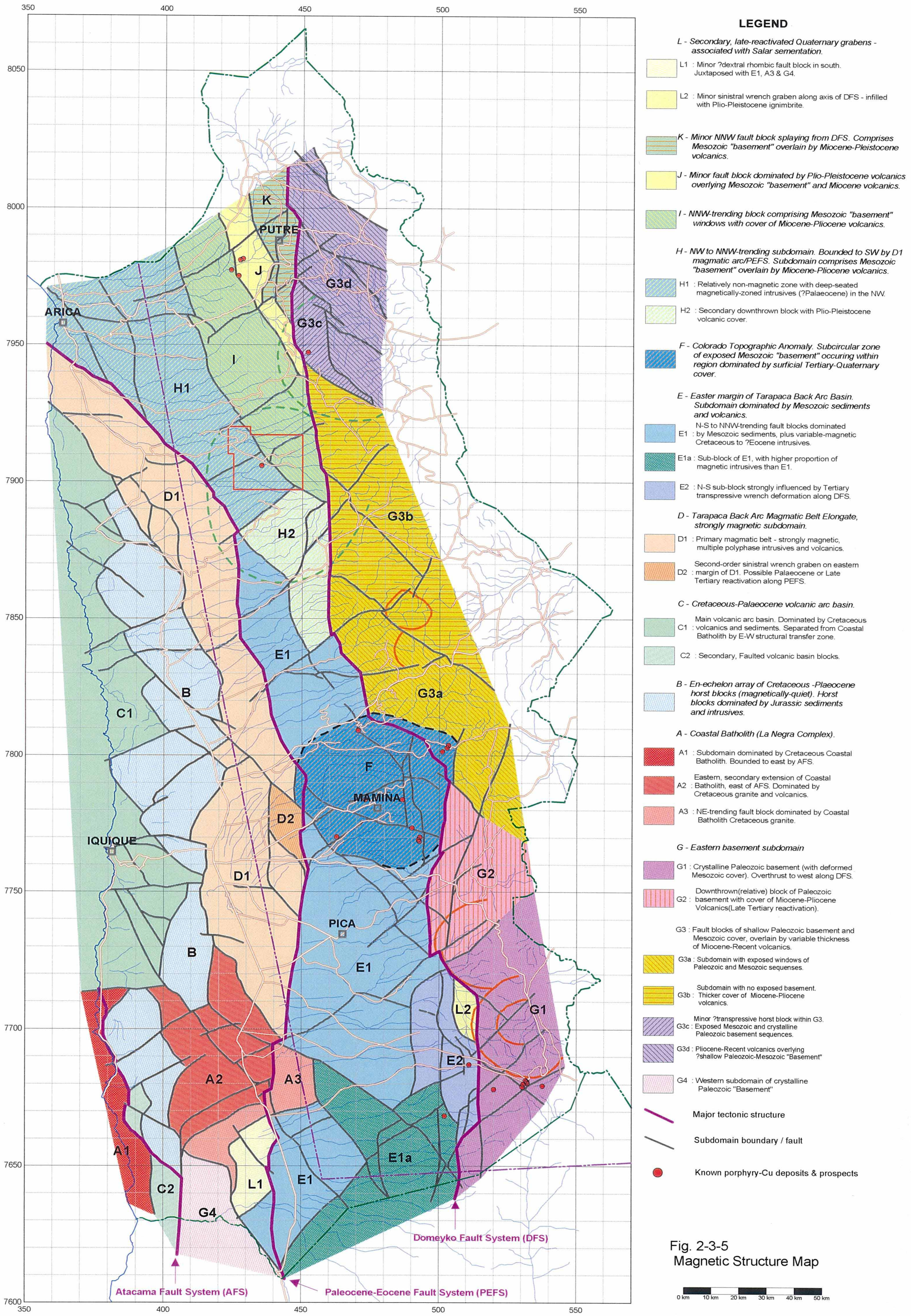

Fig. 2-3-5
Magnetic Structure Map

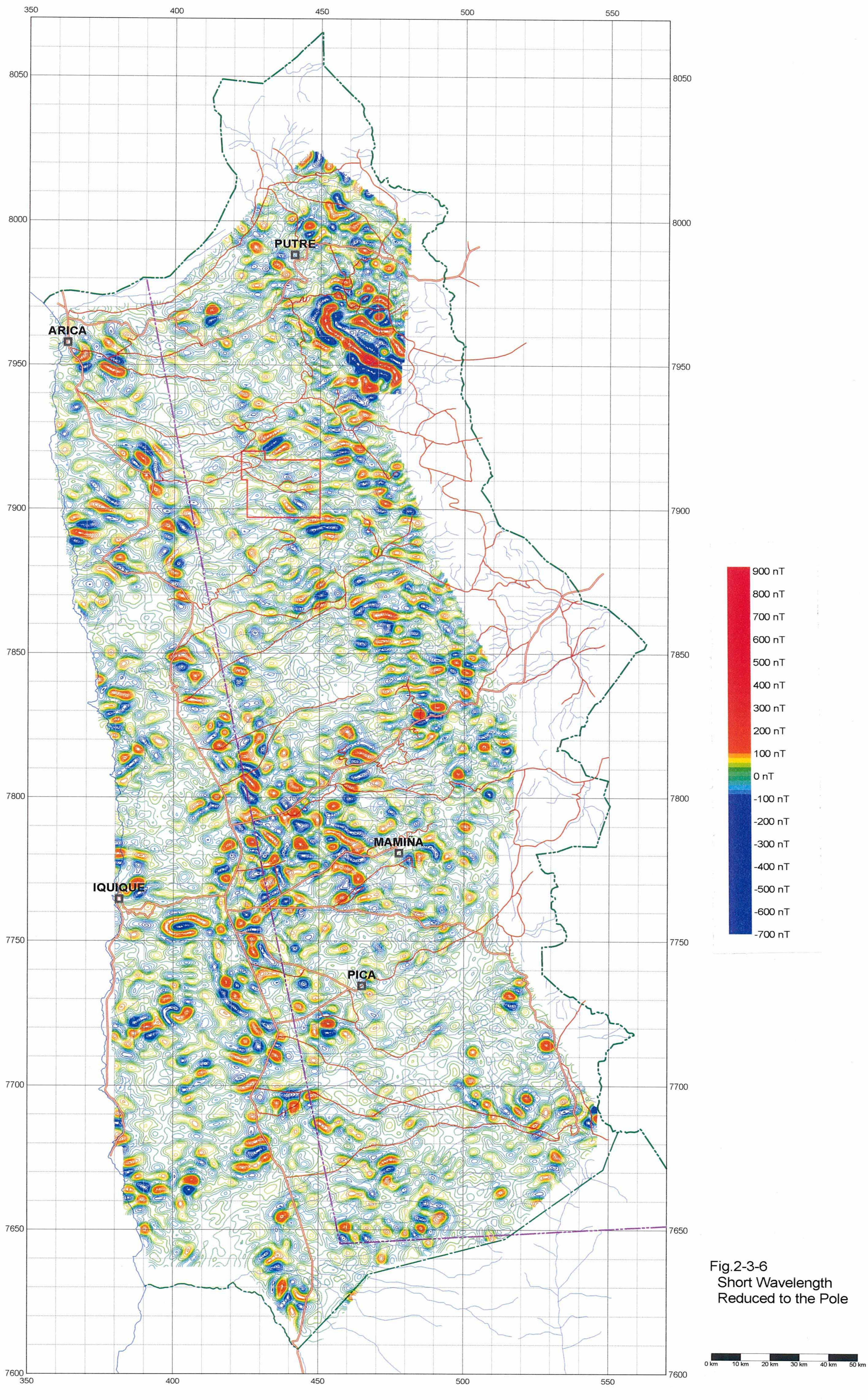

Fig.2-3-6
Short Wavelength
Reduced to the Pole

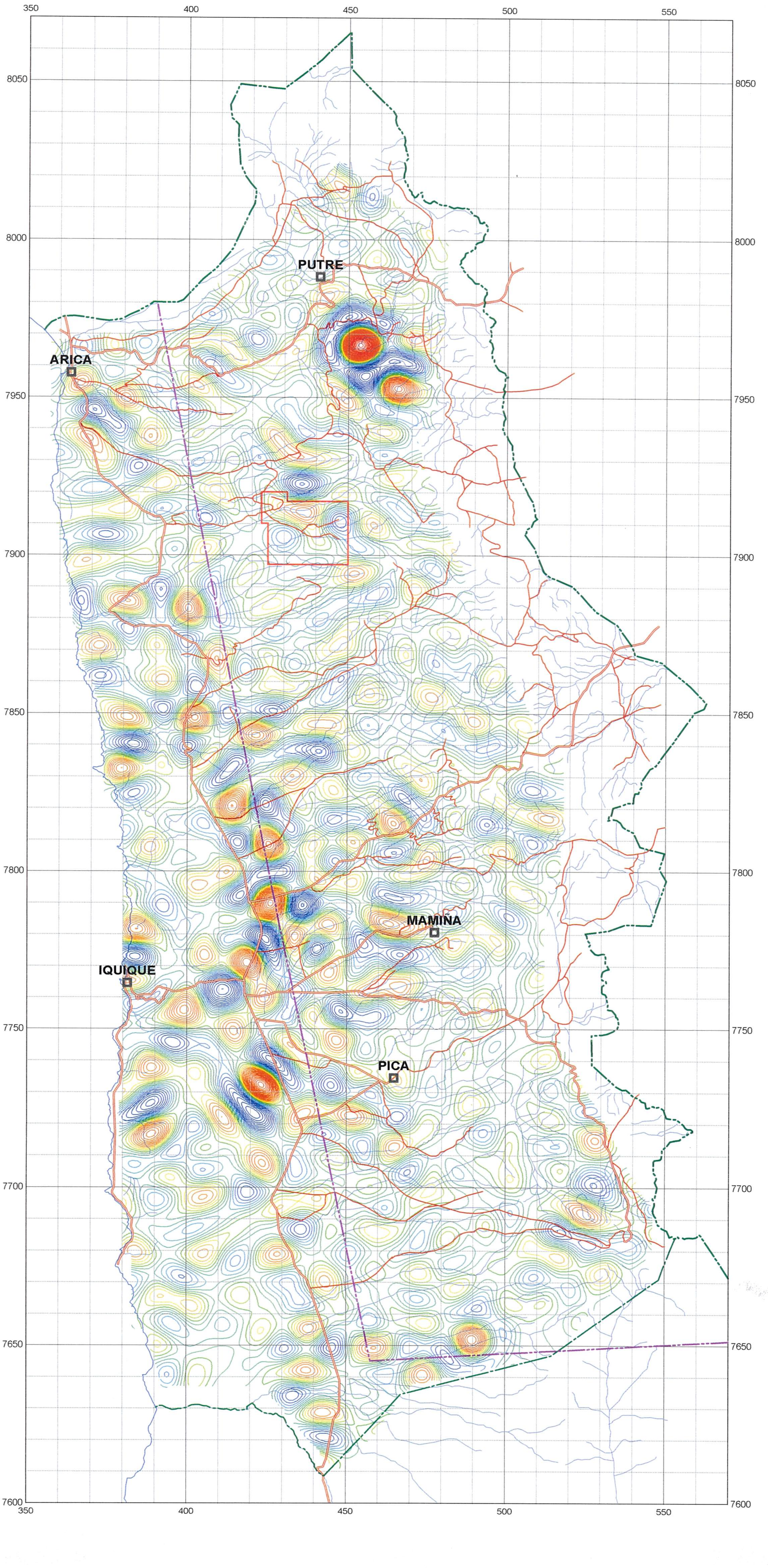

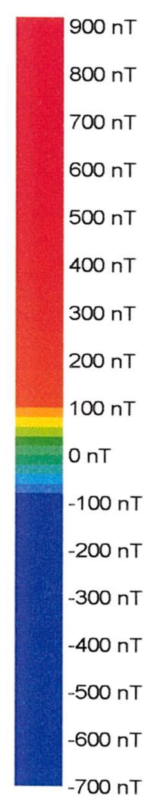

Fig.2-3-7
Medium Wavelength
Reduced to the Pole

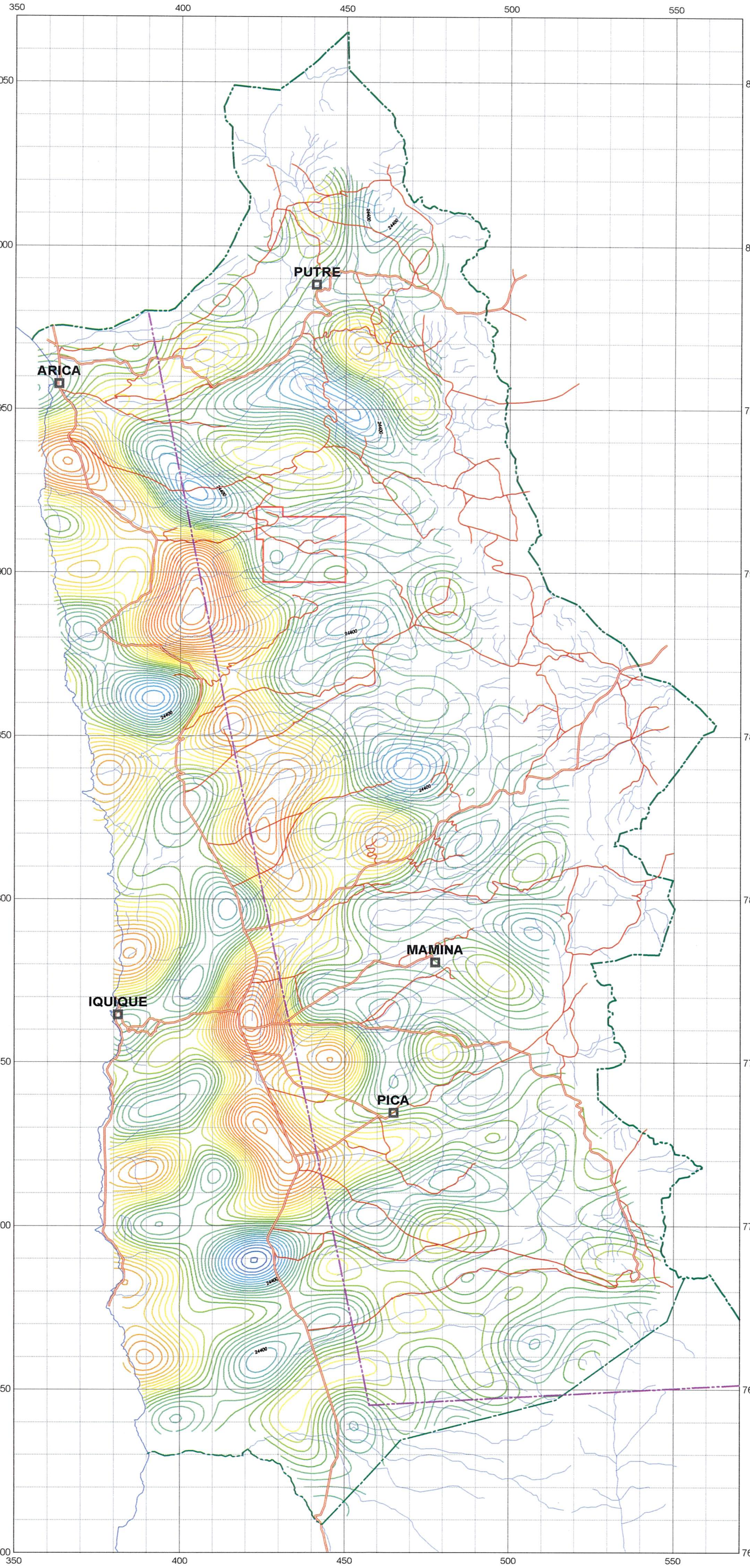

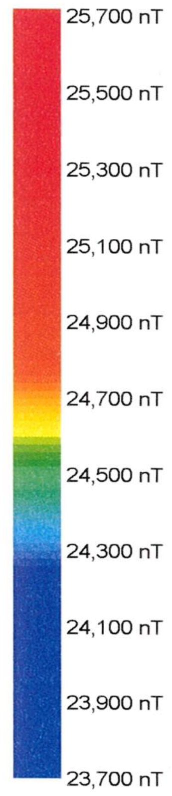

Fig.2-3-8
Long Wavelength
Reduced to the Pole